

Production of digluon and quark-antiquark dijets in central exclusive processes

Antoni Szczurek ^{1,2}

¹ Institute of Nuclear Physics PAN
PL-31-342 Cracow, Poland

² University of Rzeszów
PL-35-959 Rzeszów, Poland

We discuss exclusive central production of Higgs boson, quark-antiquark and digluon dijets. Some differential distributions are shown and discussed. Irreducible leading-order $b\bar{b}$ background to Higgs production is calculated. The signal-to-background ratio is shown and improvements are suggested by imposing cuts on b (\bar{b}) transverse momenta and rapidities. We discuss also gluonic dijet production. Here we use rather reggeon-reggeon-gluon vertices. We discuss briefly also a new mechanism of emission of gluons from different t -channel gluons (reggeons). The latter contribution turned out to be rather small. When gluons are misidentified as b or \bar{b} jets the latter contribution constitutes a reducible but large contribution to exclusive Standard Model Higgs boson.

1 Introduction

Since the cross section for exclusive Higgs boson production is rather small, only $b\bar{b}$ final state can be used in practice to identify Higgs boson. This means that a $b\bar{b}$ continuum background is of crucial importance. We discuss this irreducible background here.

In our calculations we include exact matrix elements and do full four-body calculations for all considered processes. The kinematically complete calculations allow to include any cut on kinematical variables which is very useful in order to find the Higgs boson signal.

We consider also exclusive gluonic dijet production. Such dijets have been observed experimentally by the CDF collaboration at the Tevatron ¹ and constitute a benchmark for further exclusive Higgs boson studies.

2 Formalism

A modern approach to exclusive Higgs boson production was proposed by Khoze, Martin and Ryskin ². Here we discuss this approach for exclusive production of quark-antiquark and digluon dijets.

2.1 $pp \rightarrow ppq\bar{q}$

Let us concentrate on the simplest case of the production of $q\bar{q}$ pair in the color singlet state. We do not consider the $q\bar{q}g$ contribution as it is higher order compared to the one considered here. In Refs. ^{3,4} the mechanisms for $b\bar{b}$ production shown in Fig.1 have been considered.

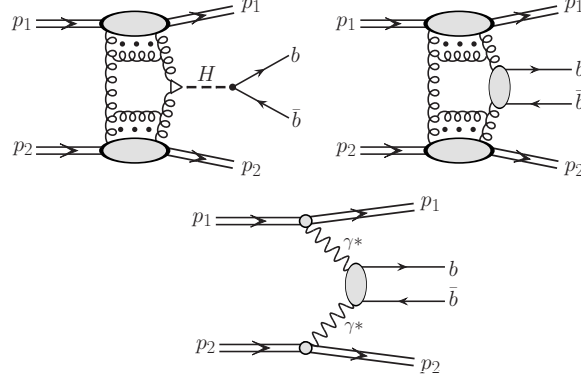


Figure 1: Diagrams included in the calculation of $b\bar{b}$ jets.

We write the amplitude of the exclusive diffractive $q\bar{q}$ pair production $pp \rightarrow p(q\bar{q})p$ in the color singlet state as

$$\mathcal{M}_{\lambda_q \lambda_{\bar{q}}}^{pp \rightarrow pp q\bar{q}}(p'_1, p'_2, k_1, k_2) = s \cdot \pi^2 \frac{1}{2} \frac{\delta_{c_1 c_2}}{N_c^2 - 1} \Im \int d^2 q_{0,t} V_{\lambda_q \lambda_{\bar{q}}}^{c_1 c_2}(q_1, q_2, k_1, k_2) \frac{f_{g,1}^{\text{off}}(x_1, x'_1, q_{0,t}^2, q_{1,t}^2, t_1) f_{g,2}^{\text{off}}(x_2, x'_2, q_{0,t}^2, q_{2,t}^2, t_2)}{q_{0,t}^2 q_{1,t}^2 q_{2,t}^2}, \quad (1)$$

where $\lambda_q, \lambda_{\bar{q}}$ are helicities of heavy q and \bar{q} , respectively. Above f_1^{off} and f_2^{off} are the off-diagonal unintegrated gluon distributions in nucleon 1 and 2, respectively. The longitudinal momentum fractions of active gluons are calculated based on kinematical variables (transverse masses and rapidities) of outgoing quark and antiquark. The bare amplitude above is subjected to absorption corrections. The absorption corrections are taken here in a simple multiplicative form.

The color singlet $q\bar{q}$ pair production amplitude can be written as⁴

$$V_{\lambda_q \lambda_{\bar{q}}}^{c_1 c_2}(q_1, q_2, k_1, k_2) \equiv n_\mu^+ n_\nu^- V_{\lambda_q \lambda_{\bar{q}}}^{c_1 c_2, \mu\nu}(q_1, q_2, k_1, k_2). \quad (2)$$

The tensorial part of the amplitude reads:

$$V_{\lambda_q \lambda_{\bar{q}}}^{\mu\nu}(q_1, q_2, k_1, k_2) = g_s^2 \bar{u}_{\lambda_q}(k_1) \left(\gamma^\nu \frac{\hat{q}_1 - \hat{k}_1 - m}{(q_1 - k_1)^2 - m^2} \gamma^\mu - \gamma^\mu \frac{\hat{q}_1 - \hat{k}_2 + m}{(q_1 - k_2)^2 - m^2} \gamma^\nu \right) v_{\lambda_{\bar{q}}}(k_2). \quad (3)$$

The coupling constants $g_s^2 \rightarrow g_s(\mu_{r,1}^2) g_s(\mu_{r,2}^2)$. In the present calculation we take the renormalization scale to be $\mu_{r,1}^2 = \mu_{r,2}^2 = M_{q\bar{q}}^2$. The exact matrix element is calculated numerically. Analytical formulae are shown explicitly in⁴.

2.2 $pp \rightarrow pp gg$

The exclusive digluon production has been discussed before in^{5,6,7}.

The mechanisms of digluon production are shown in Fig.2. The matrix element for diagrams Fig. 2 (A) and (B) to the diffractive amplitude $\mathcal{M}^{gg} = \mathcal{M}^A + \mathcal{M}^B$ for the central exclusive gg (with external color indices a and b) dijet production $pp \rightarrow p(gg)p$ can be written as⁷

$$\mathcal{M}_{ab}^A(\lambda_1, \lambda_2) = is \mathcal{A} \frac{\delta_{ab}}{N_c^2 - 1} \int d^2 \mathbf{q}_0 \frac{f_g^{\text{off}}(q_0, q_1) f_g^{\text{off}}(q_0, q_2) \cdot \epsilon_\mu^*(\lambda_1) \epsilon_\nu^*(\lambda_2)}{\mathbf{q}_0^2 \mathbf{q}_1^2 \mathbf{q}_2^2} \times \left[\frac{C_1^\mu(q_1, r_1) C_2^\nu(r_1, -q_2)}{\mathbf{r}_1^2} + \frac{C_1^\mu(q_1, r_2) C_2^\nu(r_2, -q_2)}{\mathbf{r}_2^2} \right], \quad (4)$$

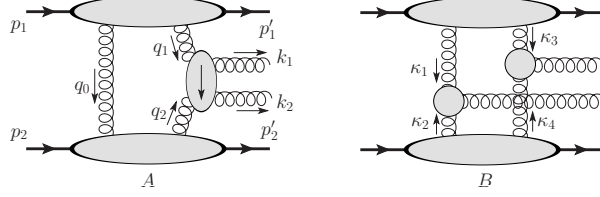


Figure 2: Mechanisms of exclusive gluonic dijet production.

$$\mathcal{M}_{ab}^B(\lambda_1, \lambda_2) = -is \mathcal{A} \frac{\delta_{ab}}{N_c^2 - 1} \int d^2 \kappa_1 \frac{f_g^{\text{off}}(\kappa_1, \kappa_3) f_g^{\text{off}}(\kappa_2, \kappa_4) \cdot \epsilon_\mu^*(\lambda_1) \epsilon_\nu^*(\lambda_2)}{\kappa_1^2 \kappa_2^2 \kappa_3^2 \kappa_4^2} \times C_1^\mu(\kappa_1, -\kappa_2) C_2^\nu(\kappa_3, -\kappa_4), \quad (5)$$

where $\mathcal{A} = 2\pi^2 g_s^2 / C_F$, the minus sign in \mathcal{M}^B comes from the difference in colour factors, $\epsilon_\mu^*(\lambda_1)$ and $\epsilon_\nu^*(\lambda_2)$ are the polarisation vectors of the final state gluons with helicities λ_1, λ_2 and momenta p_3, p_4 , respectively, $f_g^{\text{off}}(v_1, v_2)$ is the off-diagonal UGDF, which is dependent on longitudinal and transverse components of both gluons with 4-momenta v_1 and v_2 , emitted from a single proton line, and

$$r_2 = q_1 - p_4, \quad \kappa_2 = -(\kappa_1 - p_4), \quad \kappa_4 = -(\kappa_3 - p_3).$$

2.3 Off-diagonal unintegrated gluon distributions

The off-diagonal parton distributions (i=1,2) are calculated as

$$f_i^{\text{KMR}}(x_i, Q_{i,t}^2, \mu^2, t_i) = R_g \frac{d[g(x_i, k_t^2) S_{1/2}(k_t^2, \mu^2)]}{d \log k_t^2} \Big|_{k_t^2 = Q_{i,t}^2} F(t_i), \quad (6)$$

where $S_{1/2}(q_t^2, \mu^2)$ is a Sudakov-like form factor relevant for the case under consideration. It is reasonable to take a factorization scale as: $\mu_1^2 = \mu_2^2 = M_{q\bar{q}}^2, M_{gg}^2$.

The factor R_g here cannot be calculated from first principles but can be estimated in the case of off-diagonal collinear PDFs when $x' \ll x$ and $xg = x^{-\lambda}(1-x)^n$. Typically $R_g \sim 1.3 - 1.4$ at the Tevatron energy. The off-diagonal form factors are parametrized here as $F(t) = \exp(B_{\text{off}} t)$. In practical calculations we take $B_{\text{off}} = 2 \text{ GeV}^{-2}$. In evaluating f_1 and f_2 needed for calculating the amplitudes (1,5) we use different collinear distributions.

In the case of diagram B for digluon production we have to notice that we are in the ERBL region⁷. The details how to treat then unintegrated gluon distributions was discussed in detail in⁷.

3 Results

3.1 Production of $b\bar{b}$ jets

The Higgs boson differential cross sections are calculated assuming a three-body process $pp \rightarrow pHp$. Assuming full coverage for outgoing protons we construct two-dimensional distributions $d\sigma/dy d^2 p_t$ in Higgs rapidity and transverse momentum. The distribution is used then in a simple Monte Carlo code which includes the Higgs boson decay into the $b\bar{b}$ channel. It is checked whether b and \bar{b} enter into the central detector.

In Fig.3 we show the Higgs boson production cross section as a function of Higgs boson mass for different collinear gluon distributions. The cross section is rather small.

In the left panel of Fig.4 we show the central diffractive contribution for CTEQ6⁸ collinear gluon distribution and the contribution from the decay of the Higgs boson including natural

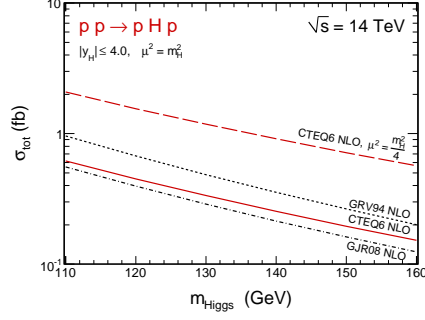


Figure 3: Total cross section as a function of Higgs boson mass.

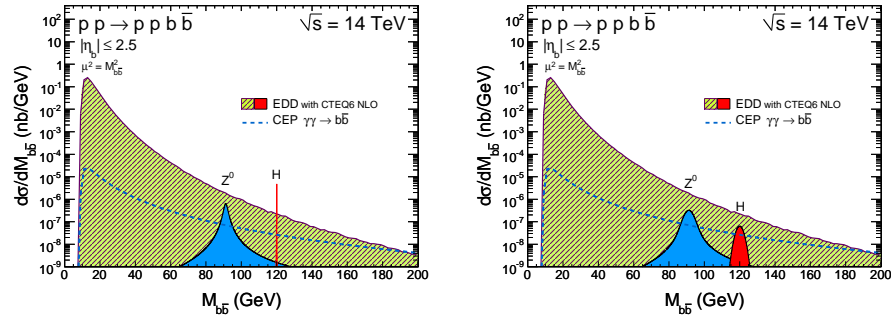


Figure 4: The $b\bar{b}$ invariant mass distribution for $\sqrt{s} = 14$ TeV and for b and \bar{b} jets for $-2.5 < \eta < 2.5$ corresponding to the ATLAS detector. The left panel shows purely theoretical predictions, while the right panel includes experimental effects due to experimental uncertainty in missing mass measurement.

decay width, see the sharp peak at $M_{b\bar{b}} = 120$ GeV. The phase space integrated cross section for the Higgs production, including absorption effects with gap survival probability $S_G = 0.03$ is less than 1 fb. The result shown in Fig.4 includes branching fraction for $\text{BR}(H \rightarrow b\bar{b}) \approx 0.8$ and the rapidity restrictions. The much broader Breit-Wigner type peak to the left of the Higgs signal corresponds to the exclusive production of the Z^0 boson with the cross section calculated as in Ref. ¹⁰. The branching fraction $\text{BR}(Z^0 \rightarrow b\bar{b}) \approx 0.15$ has been included in addition. In contrast to the Higgs case the absorption effects for the Z^0 production are much smaller ¹⁰. The sharp peak corresponding to the Higgs boson clearly sticks above the background.

In Refs.^{3,4} we have discussed in great detail how to improve the difficult situation. Examples are shown in Fig.5. In all considered cases the situation seems much better. We have checked, however, that this is an optimal situation and further improvement of the signal-to-background ratio is not possible.

3.2 Digluon production

The dijet production has been measured by the CDF collaboration at the Tevatron ¹. In Fig.6 we show the experimental data together with our predictions. We get a good description of the data within model uncertainties. We find that the quark-antiquark contribution is more than three orders of magnitude smaller than the digluon one.

In Fig.7 we present invariant mass distribution. We compare contribution of the two mechanisms shown in Fig.2. The contribution of the diagram B depends strongly on the power of (collinear) gluon distribution at low- x . It is clear that its contribution at larger invariant masses is completely negligible.

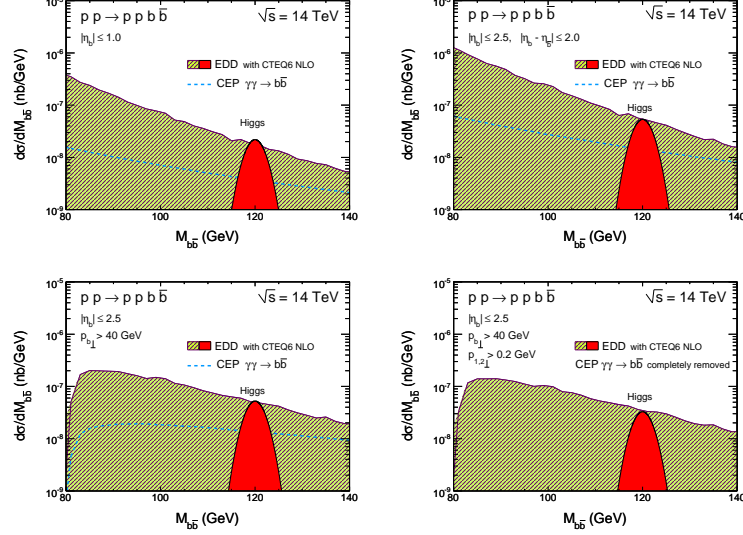


Figure 5: Invariant mass distribution of the $b\bar{b}$ dijets. Here experimental resolution on pp missing mass has been included. The Gaussian-type line (area) corresponds to the Standard Model Higgs boson production. Shown are results with different combinations of cuts which can be used to improve the signal-to-background ratio.

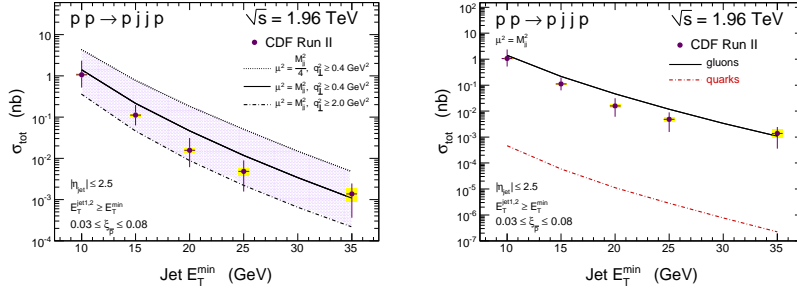


Figure 6: Cross section as a function of the lower cut on jet transverse energy. The left panel shows uncertainties on the choice of scales while the right panel compares the digluon and quark-antiquark components.

In Ref.⁷ we have discussed also a formally reducible background of the gluonic dijets to the Higgs boson production. This contribution is similar to that for the $b\bar{b}$ continuum discussed also in this presentation above. In Fig.8 we show an example of the reducible background with some set of cuts. Large contribution of the reducible background has been found.

4 Conclusions

We have shown and discussed differential distributions for the continuum $b\bar{b}$ production. The corresponding amplitude has been calculated in the Khoze-Martin-Ryskin approach.

The $b\bar{b}$ continuum constitutes irreducible background for exclusive Higgs boson production. Experimental resolution on pp missing mass has been included when comparing the Higgs signal and the $b\bar{b}$ background. Our analysis shows that a special cuts can be useful to see the Standard Model Higgs boson signal.

We have discussed also production of gluonic dijets. In our approach to corresponding matrix element has been calculated using rather Lipatov reggeon-reggeon-gluon vertices. We have considered a new mechanism when gluons are emitted from different t -channel gluons (reggeons). The contribution of the latter mechanism turned out to be rather small.

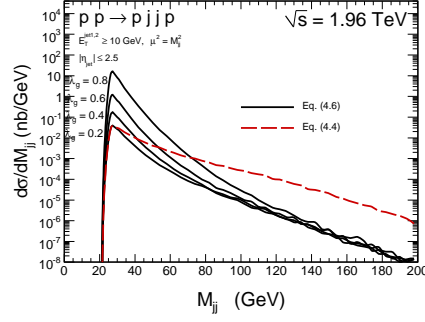


Figure 7: Invariant mass distribution of gluonic dijets.

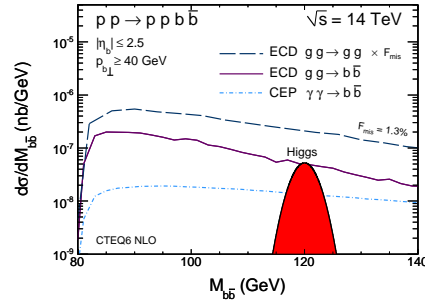


Figure 8: Invariant mass distribution of the $b\bar{b}$ system. Shown are contributions from diffractive Higgs boson (shaded area), $b\bar{b}$ continuum (solid line), $\gamma\gamma$ continuum (dash-dotted line) and diffractive digluon contribution (dashed line) multiplied by an ATLAS misidentification factor squared.

When gluons are misidentified as b (\bar{b}) jets the exclusive digluon continuum constitutes a reducible background to exclusive Higgs boson production. We have shown that this background is comparable to the irreducible $b\bar{b}$ continuum.

Our analysis indicates that a real experiment can be rather difficult. The situation could be better for some scenarios beyond the Standard Model^{11,12}.

I am indebted to Rafał Maciuła and Roman Pasechnik for collaboration on the issues presented here. I congratulate the organizers, Tran Thanh Vahn, Chung-I Tan and Mary Rotondo, for very good organization and friendly atmosphere during the Blois workshop in Quy Nhon.

1. T. Aaltonen *et al.* [CDF Collaboration], Phys. Rev. D **77**, 052004 (2008);
A. A. Affolder *et al.* [CDF Collaboration], Phys. Rev. Lett. **88**, 151802 (2002);
A. A. Affolder *et al.* [CDF Collaboration], Phys. Rev. Lett. **85**, 4215 (2000).
2. V. A. Khoze, A. D. Martin and M. G. Ryskin, Phys. Lett. B **401**, 330 (1997);
A. B. Kaidalov, V. A. Khoze, A. D. Martin and M. G. Ryskin, Eur. Phys. J. C **33**, 261 (2004).
3. R. Maciuła, R. Pasechnik and A. Szczurek, arXiv:1006.3007 [hep-ph], Phys. Rev. **D82** 114011 (2010).
4. R. Maciuła, R. Pasechnik and A. Szczurek, arXiv:1011.5842 [hep-ph], Phys. Rev. **D83** 114034 (2011).
5. J. R. Cudell, A. Dechambre, O. F. Hernandez and I. P. Ivanov, Eur. Phys. J. C **61**, 369 (2009).
6. A. Dechambre, O. Kepka, C. Royon and R. Staszewski, Phys. Rev. D **83**, 054013 (2011) [arXiv:1101.1439 [hep-ph]].

7. R. Maciula, R. Pasechnik and A. Szczurek, arXiv:1109.5517 [hep-ph], Phys. Rev. **D84** 114014 (2011).
8. J. Pumplin et al., JHEP 0207, 012 (2002).
9. V. S. Fadin and L. N. Lipatov, Sov. J. Nucl. Phys. **50**, 712 (1989) [Yad. Fiz. **50**, 1141 (1989)].
10. A. Cisek, W. Schäfer and A. Szczurek, Phys. Rev. **D80** 074013 (2009).
11. B. E. Cox, F. K. Loebinger, A. D. Pilkington, JHEP **0710**, 090 (2007).
12. S. Heinemeyer, V.A. Khoze, M.G. Ryskin, W.J. Stirling, M. Tasevsky, and G. Weiglein, Eur. Phys. J. C **53** 231 (2008).

